

## Role of Au–C Interactions on the Catalytic Activity of Au Nanoparticles Supported on TiC(001) toward Molecular Oxygen Dissociation

José A. Rodríguez,<sup>\*,†</sup> Leticia Feria,<sup>‡</sup> Tomas Jirsak,<sup>†</sup> Yoshiro Takahashi,<sup>§</sup> Kenichi Nakamura,<sup>§</sup> and Francesc Illas<sup>\*,‡</sup>

*Chemistry Department, Brookhaven National Laboratory, Upton, New York 11973, Departament de Química Física & Institut de Química Teòrica i Computacional (IQTCUB), Universitat de Barcelona, C/Martí i Franquès 1, 08028 Barcelona, Spain, and Materials and Structures Laboratory, Tokyo Institute of Technology, Yokohama 226-8503, Japan*

Received December 1, 2009; E-mail: rodriguez@bnl.gov; francesc.illas@ub.edu

**Abstract:** High-resolution photoemission and density functional calculations on realistic slab surface models were used to study the interaction and subsequent dissociation of O<sub>2</sub> with Au nanoparticles supported on TiC(001). The photoemission results indicate that at 150 K O<sub>2</sub> adsorbs molecularly on the supported gold nanoparticles, and upon heating to temperatures above 200 K the O<sub>2</sub> → 2O reaction takes place with migration of atomic oxygen to the TiC(001) substrate. The addition of Au to TiC(001) substantially enhances the rate of O<sub>2</sub> dissociation at room temperature. The reactivity of Au nanoparticles supported on TiC(001) toward O<sub>2</sub> dissociation is much larger than that of similar nanoparticles supported either on TiO<sub>2</sub>(110) or MgO(001) surfaces, where the cleavage of O–O bonds is very difficult. Density functional calculations carried out on large supercells show that the contact of Au with TiC(001) is essential for charge polarization and an enhancement in the chemical activity of Au. Small two-dimensional particles which expose Au atoms in contact with TiC(001) are the most reactive. While O<sub>2</sub> prefers binding to Au sites, the O atoms interact more strongly with the TiC(001) surface. The oxygen species active during the low-temperature (<200 K) oxidation of carbon monoxide on Au/TiC(001) is chemisorbed O<sub>2</sub>. Once atomic O binds to TiC(001), the chemisorption bond is so strong that temperatures well above 400 K are necessary to remove the O adatoms from the TiC(001) substrate by direct reaction with CO. The high reactivity of Au/TiC(001) toward O<sub>2</sub> at low-temperature opens the route for the transformation of alcohols and amines on the supported Au nanoparticles.

### I. Introduction

Among the transition metals, bulk metallic gold is by far the least reactive.<sup>1–10</sup> Typically a Au(111) surface has an extremely low catalytic activity,<sup>3–5</sup> but the addition of oxygen adatoms produces systems with quite interesting chemical properties.<sup>4–10</sup> In the last 10 years, gold nanoparticles supported on oxides have

become the subject of considerable attention due to their high activity for the oxidation of carbon monoxide (2CO + O<sub>2</sub> → 2CO<sub>2</sub>) at relatively low temperatures (200–350 K).<sup>11–21</sup> This phenomenon was originally discovered by Haruta and co-workers in the early 1990s<sup>11</sup> and has been corroborated by many subsequent studies.<sup>12,17,19–21</sup> The exact catalytic activity of the Au/oxide system depends on the method of preparation, the nature of the oxide, and the dispersion of the metal on the support.<sup>11,17,19–21</sup> In general, Au particles with sizes between 1 and 3 nm display catalytic activity for CO oxidation much larger than that of bulk metallic gold.<sup>11,19–21</sup>

<sup>†</sup> Brookhaven National Laboratory.

<sup>‡</sup> Universitat de Barcelona.

<sup>§</sup> Tokyo Institute of Technology.

- (1) Thomas, J. M.; Thomas, W. J. *Principles and Practice of Heterogeneous Catalysis*; VCH: New York, 1997.
- (2) Gates, B. C. *Catalytic Chemistry*; Wiley: New York, 1992.
- (3) Hammer, B.; Nørskov, J. K. *Nature* **1995**, *376*, 238.
- (4) Min, B. K.; Friend, C. M. *Chem. Rev.* **2007**, *107*, 2709.
- (5) Liu, X.; Xu, B.; Haubrich, J.; Madix, R. J.; Friend, C. M. *J. Am. Chem. Soc.* **2009**, *131*, 5757.
- (6) Ojifinni, R. A.; Froemming, N. S.; Gong, J.; Pan, M.; Kim, T. S.; White, J. M.; Henkelman, G.; Mullins, C. B. *J. Am. Chem. Soc.* **2008**, *130*, 6801.
- (7) Gong, J.; Ojifinni, R. A.; Kim, T. S.; White, J. M.; Mullins, C. B. *J. Am. Chem. Soc.* **2006**, *128*, 9012.
- (8) Ojifinni, R. A.; Gong, J.; Froemming, N. S.; Flaherty, D. W.; Pan, M.; Henkelman, G.; Mullins, C. B. *J. Am. Chem. Soc.* **2008**, *130*, 11250.
- (9) Kim, T. S.; Gong, J.; Ojifinni, R. A.; White, J. M.; Mullins, C. B. *J. Am. Chem. Soc.* **2006**, *128*, 6282.
- (10) Gong, J. L.; Mullins, C. B. *J. Am. Chem. Soc.* **2008**, *130*, 16458.

- (11) Haruta, M. *Catal. Today* **1997**, *36*, 153.
- (12) Chen, M. S.; Goodman, D. W. *Science* **2004**, *306*, 252.
- (13) Campbell, C. T.; Parker, S. C.; Starr, D. E. *Science* **2002**, *298*, 811.
- (14) Molina, L. M.; Hammer, B. *Appl. Catal. A: Gen.* **2005**, *291*, 21.
- (15) Vijay, A.; Mills, G.; Metiu, H. *J. Chem. Phys.* **2003**, *118*, 6536.
- (16) Remediakis, I. N.; Lopez, N.; Nørskov, J. K. *Angew. Chem., Int. Ed.* **2005**, *117*, 1858.
- (17) Guzman, J.; Carrettin, S.; Fierro-Gonzalez, J. C.; Hao, Y.; Gates, B. C.; Corma, A. *Angew. Chem. Int. Ed.* **2005**, *117*, 4856.
- (18) Cruz Hernández, N.; Sanz, J. F.; Rodriguez, J. A. *J. Am. Chem. Soc.* **2006**, *128*, 15600.
- (19) Walden, M.; Lai, X.; Goodman, D. W. *Science* **1998**, *281*, 1647.
- (20) Meerson, O.; Sitja, G.; Henry, C. R. *Eur. Phys. J. D.* **2005**, *34*, 119.
- (21) Rodriguez, J. A. *Dekker Encyclopedia of Nanoscience and Nanotechnology*; Dekker: New York, 2004; pp 1297–1304.

The catalytic activity of supported Au nanoparticles has been attributed to various effects, such as the presence of low-coordinated atoms, electronic confinement, particle shape, fluxionability, and interactions with the support.<sup>11–22</sup> A very important issue is the adsorption and dissociation of O<sub>2</sub> on the Au/oxide systems, since this seems to be a necessary step in total and partial oxidation reactions.<sup>4–10</sup> Can isolated Au nanoparticles dissociate O<sub>2</sub>?<sup>15,16,23,24</sup> Is the Au–oxide interface necessary for the cleavage of O–O bonds?<sup>14–17,25</sup> Calculations based on density functional theory have been carried out for a series of unsupported Au nanoparticles as well as for extended systems containing low-coordinated sites.<sup>23</sup> This systematic study has shown that, contrarily to the case of H<sub>2</sub> dissociation by Au,<sup>26</sup> the presence of low-coordinate Au atoms is not enough to dissociate O<sub>2</sub>. Strong adsorption of molecular oxygen on Au nanoparticles is a necessary but not sufficient condition for O<sub>2</sub> dissociation.<sup>23</sup> For reasonably large Au cuboctahedral nanoparticles, there is a common pathway for O<sub>2</sub> dissociation on nanoparticles that involves a particular configuration of adsorption sites and a critical particle size.<sup>23</sup> If these conditions are not satisfied, the oxidation of CO on gold/oxide systems probably follows a mechanism in which the cleavage of the O–O bond in molecular oxygen is facilitated by interactions with the CO molecule (i.e., O–O•••C–O → O + CO<sub>2</sub>).<sup>14,16,18</sup>

There is a general desire to find supports that can activate gold up to the point that this metal easily dissociates O<sub>2</sub>.<sup>21,23,27</sup> Once oxygen is present on a gold surface, the system reacts readily with CO, CO<sub>2</sub>, NH<sub>3</sub>, H<sub>2</sub>O, CH<sub>3</sub>OH, CH<sub>3</sub>CH<sub>2</sub>OH, and CH<sub>3</sub>CH<sub>2</sub>CH<sub>2</sub>OH.<sup>4–10</sup> What happens when Au is deposited on a substrate that has physical and chemical properties that differ from those of an oxide? The carbides of the early transition metals exhibit, in many aspects, a chemical behavior similar to that of noble metals.<sup>28,29</sup> A recent paper indicates that Au particles dispersed on TiC can oxidize carbon monoxide at temperatures below 200 K.<sup>30</sup> In a subsequent study, high-resolution photoemission, scanning tunneling microscopy (STM), and first-principles density-functional (DF) slab calculations were used to study the adsorption of gold on a TiC(001) surface.<sup>31</sup> The Au↔TiC(001) interactions were found to be much stronger than typical Au↔oxide interactions. Both, the photoemission and DF results point to the formation of Au–C bonds. In general, the bond between Au and the TiC(001) surface exhibits very little ionic character but displays a substantial polarization of electrons around Au,<sup>31</sup> which enhances the chemical activity of this metal.<sup>32,33</sup>

In this paper, we investigate the adsorption and dissociation of O<sub>2</sub> on Au/TiC(001) surfaces using high-resolution photoemission and DF calculations. We find that the addition of small Au nanoparticles to TiC(001) clearly enhances the dissociation rate of O<sub>2</sub>. We find that the Au/TiC(001) system is more active for the cleavage of O–O bonds than any Au/oxide system reported in the literature. Furthermore, very high activity for the dissociation of O<sub>2</sub> is seen only for small two-dimensional gold clusters in close contact with the titanium carbide substrate, when the effects of Au–C interactions are very strong. Implications for the oxidation of CO on Au/TiC(001) and the transformation of alcohols are also discussed.

## II. Experimental and Theoretical Methods

**A. Photoemission and Thermal-Desorption Experiments.** The photoemission studies for the adsorption of oxygen on Au/TiC(001) were performed at the U7A beamline of the National Synchrotron Light Source (NSLS) at Brookhaven National Laboratory (BNL). This beamline is equipped with a conventional ultrahigh-vacuum (UHV) chamber (base pressure  $\sim 5 \times 10^{-10}$  Torr) that contains a hemispherical electron energy analyzer with multichannel detection, instrumentation for low-energy electron diffraction (LEED), a quadrupole mass spectrometer, and a dual anode Mg/Al K $\alpha$  X-ray source.<sup>31–34</sup> The Au 4f, C 1s, Ti 2p, and O 1s spectra reported in section III were recorded using photon energies of 380, 380, 550, and 625 eV, respectively.<sup>33</sup> At these photon energies, photoemission probed only the composition of the first two or three layers of the sample. The overall instrumental energy resolution in the photoemission experiments was  $\sim 0.3$  eV. The binding energy scale in the photoemission spectra was calibrated by the position of the Fermi edge in the valence region. Additional experiments were performed at two UHV chambers (base pressure  $< 3 \times 10^{-10}$  Torr) located at the Tokyo Institute of Technology (TIT) with capabilities for X-ray photoelectron spectroscopy (Al K $\alpha$  X-ray source), LEED, Auger electron spectroscopy (AES), thermal-desorption mass spectroscopy (TDS), and scanning tunneling microscopy (STM).<sup>32,33</sup>

In the UHV chambers at BNL and TIT, the TiC(001) crystal was mounted and cleaned following the methodology described elsewhere.<sup>35,36</sup> The cleaning procedure led to a clear  $1 \times 1$  diffraction pattern in LEED and no surface impurities in photoemission or XPS. The crystal growers estimated a TiC<sub>0.95–0.98</sub> stoichiometry for the bulk of the sample, and after cleaning our quantitative XPS results showed surfaces with essentially a Ti/C ratio of 1.<sup>31,35,36</sup> For surfaces prepared in this way, images of scanning tunneling microscopy (STM) give a square crystal lattice with terraces that are 400–550 Å wide, separated by single and double step heights.<sup>32,33</sup>

The Au/TiC(001) systems were prepared following the methodology used in our previous studies with these systems.<sup>31–33</sup> Molecular oxygen (99.995% purity) was dosed to the Au/TiC(001) surfaces at 150 or 300 K using dosing tubes with apertures located  $\sim 5$  mm away from the sample. These dosing systems provided a large enhancement ( $>10$  times) in the mass adsorbed with respect to dosing by backfilling the UHV chambers with O<sub>2</sub>. The reported exposures of O<sub>2</sub> are based on the direct ion gauge readings without correction for the enhancement factors of the dosers.

**B. First-Principles Density Functional Calculations.** The adsorption of O<sub>2</sub> on Au/TiC(001) model systems has also been studied by means of calculations based on Density Functional Theory, within the usual Kohn–Sham formalism, carried out for suitable periodic representations of these systems. The PW91 form of the generalized gradient approximation (GGA) has been chosen

- (22) Boronat, M.; Concepción, P.; Corma, A.; González, S.; Illas, F.; Serna, P. *J. Am. Chem. Soc.* **2007**, *129*, 16230.  
 (23) Roldan, A.; Gonzalez, S.; Ricart, J. M.; Illas, F. *Chem. Phys. Chem.* **2009**, *10*, 348.  
 (24) Barrio, L.; Liu, P.; Rodriguez, J. A.; Campos-Martin, J. M.; Fierro, J. L. G. *J. Phys. Chem. C* **2007**, *111*, 19001.  
 (25) Turner, M.; Golovko, V. B.; Vaughan, O. P. H.; Abdulkin, P.; Berenguer-Murcia, A.; Tikhov, M. S.; Johnson, B. F. G.; Lambert, R. M. *Nature* **2008**, *454*, 981.  
 (26) Corma, A.; Boronat, M.; González, S.; Illas, F. *Chem. Commun.* **2007**, 3371.  
 (27) Herzog, A. A.; Kiely, C. J.; Carley, A. F.; Landon, P.; Hutchings, G. J. *Science* **2008**, *321*, 1331.  
 (28) Hwu, H.; Chen, J. G. *Chem. Rev.* **2005**, *105*, 185.  
 (29) Levy, R. B.; Boudart, M. *Science* **1973**, *181*, 547.  
 (30) Ono, L. K.; Sudfeld, D.; Roldan Cuenya, B. *Surf. Sci.* **2006**, *600*, 5041.  
 (31) Rodríguez, J. A.; Viñes, F.; Illas, F.; Liu, P.; Takahashi, Y.; Nakamura, K. *J. Chem. Phys.* **2007**, *127*, 211102.  
 (32) Rodríguez, J. A.; Liu, P.; Viñes, F.; Illas, F.; Takahashi, Y.; Nakamura, K. *Angew. Chem., Int. Ed.* **2008**, *47*, 6685.  
 (33) Rodríguez, J. A.; Liu, P.; Viñes, F.; Illas, F.; Takahashi, Y.; Nakamura, K. *J. Am. Chem. Soc.* **2009**, *131*, 8592.

- (34) Rodríguez, J. A.; Liu, P.; Dvorak, J.; Jirsak, T.; Gomes, J.; Takahashi, Y.; Nakamura, K. *J. Chem. Phys.* **2004**, *121*, 465.  
 (35) Frantz, P.; Didziulis, S. V. *Surf. Sci.* **1998**, *412/413*, 384.  
 (36) Frantz, P.; Didziulis, S. V.; Merrill, P. B.; Pery, S. S.; El-bjerami, O.; Imaduddin, S. *J. Phys. Chem. B* **1999**, *103*, 11129.

for the exchange-correlation potential.<sup>37</sup> The effect of the atomic cores on the valence electron density has been taken into account by means of the projected augmented plane-wave (PAW) method of Blöchl,<sup>38</sup> as implemented by Kresse and Joubert<sup>39</sup> in the VASP code.<sup>40,41</sup> This representation of the core states allows one to obtain converged results with a cutoff kinetic energy of 415 eV for the plane wave basis set. The Monkhorst–Pack scheme<sup>42</sup> has been used to select the special *k*-points used to carry out the numerical integrations in the reciprocal space. A conjugated gradient algorithm with an energy criterion of 0.001 eV has been used for the atomic convergence, which ensured forces to be in all cases smaller than 0.03 eV/Å.

The TiC(001) surface has been modeled by slab models repeated periodically with a vacuum region of 10 Å between repeated slabs. The slabs were constructed using the lattice parameter optimized for the bulk of TiC and reported in a previous work.<sup>43</sup> They all contained four atomic layers but different surface area. In all cases the two outermost layers of one side of the slab were completely allowed to relax. Au<sub>2</sub>, Au<sub>4</sub>, Au<sub>13</sub>, and Au<sub>29</sub> clusters and a Au monolayer were set above the TiC(001) surface as described previously and the vacuum space enlarged accordingly to maintain the repeated slabs enough away from each other.<sup>31–33</sup> For Au<sub>2</sub> and Au<sub>4</sub>, the Au atoms were placed initially above C atoms. Au<sub>13</sub> contains two atomic layers with nine and four atoms, respectively. The atoms in the bottom layer are initially located above the C atoms of the TiC substrate and those on the second layer at the 4-fold hollow sites. Finally, Au<sub>29</sub> contains three atomic layers with 16, 9, and 4 atoms, respectively, with the 16 atoms at the base of the truncated square pyramid initially above C atoms as for the rest of Au particles discussed above. Nevertheless, the structure of the supported particle was always fully optimized allowing the two uppermost atomic layers of the TiC substrate to relax. This type of geometry optimization was also carried out in the series of calculations where the O<sub>2</sub> molecule interacts with the Au-supported particles.

Because of the different size of the Au nanoparticles studied in the present work, it is necessary to use different supercells to simulate an adequate and comparable Au nanoparticle coverage and thus dispersion of supported particles while at the same time ensuring that the interaction between supported particles is negligible.<sup>44,45</sup> Thus, for Au<sub>2</sub> on TiC we used a 2 × 2 cubic unit cell containing a total of 66 (64 TiC + 2 Au) atoms and representing a coverage of 0.125 metal monolayers (ML) with respect to the number of Ti and C surface atoms. For supported Au<sub>4</sub>, we used a 3 × 3 unit cell (144 + 4 atoms) with a resulting coverage of 0.111 ML, whereas for supported Au<sub>13</sub> and Au<sub>29</sub> 5 × 5 (400 + 13 atoms) and 6 × 6 (576 + 29 atoms) were employed, respectively, with coverage of 0.130 and 0.201 ML. For the Au monolayer we used the 2 × 2 unit cell but with eight Au atoms on the surface resulting in a 0.5 ML coverage. In each case, a suitable Monkhorst–Pack of special *k* points has been used: 5 × 5 × 1 for the 2 × 2 unit cell and 3 × 3 × 1 for the 3 × 3 unit cell. Calculations for the 5 × 5 and 6 × 6 unit cells were carried out at the  $\Gamma$  point. The present models of supported Au nanoparticles are realistic enough to provide a meaningful comparison with experiment. It is worth pointing out that calculations for the largest supported particles, involving explicitly 605 atoms and full relaxation of 317 atoms, are computationally very demanding, thus requiring access to large supercomputers. To the best of our knowledge, this is the first time

where explicit exploration of the potential energy surface and appropriate characterization of stationary points (minima and TS structures including support relaxation) has been carried out for rather large isolated supported metal nanoparticles.

Once the final geometries were obtained for the O<sub>2</sub>/Au/TiC(001) systems, a proper vibrational analysis has been used to characterize final geometries as minimum energy structures and the corresponding adsorption energies calculated as

$$E_{\text{ads}} = -\{E_{\text{O}_2/\text{AuTiC}} - (E_{\text{O}_2} + E_{\text{AuTiC}})\} \quad (1)$$

where  $E_{\text{O}_2}$  is the spin polarized energy of the isolated O<sub>2</sub> molecule,  $E_{\text{AuTiC}}$  is the total energy of the relaxed Au/TiC(001) surface, and  $E_{\text{O}_2/\text{AuTiC}}$  is the energy of the Au/TiC(001) surface with O<sub>2</sub> adsorbed. Transition state structures for O<sub>2</sub> dissociation were located with the help of the climbing image nudged elastic band (CI-NEB)<sup>46,47</sup> or of the dimer<sup>48</sup> algorithms as implemented in VASP and properly characterized by vibrational analysis. We already mentioned that, in all calculations, the atomic structure and location of the supported particle, the position of the O atoms and that of the atoms on the two upper atomic layers of the TiC substrate were fully relaxed. However, the vibrational analysis is restricted to the degrees of freedom of the O atoms. The activation energy barriers for O<sub>2</sub> dissociation have been calculated as

$$E_{\text{act}} = -\{E_{\text{O}\cdots\text{O}/\text{AuTiC}} - (E_{\text{O}_2} + E_{\text{AuTiC}})\} \quad (2)$$

where  $E_{\text{O}_2}$  and  $E_{\text{AuTiC}}$  are as in eq 1 and  $E_{\text{O}\cdots\text{O}/\text{AuTiC}}$  is the energy of the transition state structure.

### III. Results and Discussion

**A. Adsorption and Dissociation of O<sub>2</sub> on Au/TiC(001): Photoemission Studies.** At 100 and 300 K, the sticking coefficient of O<sub>2</sub> on clean TiC(001) is low.<sup>34,35</sup> DF calculations show a relatively small adsorption energy for the O<sub>2</sub> molecule ( $E_{\text{ads}} \sim 0.45$  eV).<sup>49,50</sup> After the cleavage of the O–O bond, the O atoms bind quite strongly ( $E_{\text{ads}} \sim 5.8$  eV) to the TiC(001) surface.<sup>34,51</sup> Photoemission results show that atomic oxygen is present on the TiC(001) substrate after dosing O<sub>2</sub> at room temperature.<sup>34</sup> A big positive shift (1.5–1.8 eV) was detected for the C 1s core level.<sup>34</sup> The photoemission studies suggest the existence of strong O $\leftrightarrow$ C interactions, a phenomenon corroborated by the results of DF calculations, which show a CTiTi hollow as the most stable site for the adsorption of O.<sup>34,51</sup> Ti and C atoms are involved in the adsorption and dissociation of the O<sub>2</sub> molecule on TiC(001).<sup>34,51</sup>

The top panel in Figure 1 shows an O 1s core-level spectrum ( $h\nu = 625$  eV) taken after dosing molecular oxygen to a TiC(001) surface precovered with 0.2 ML of Au at 150 K. The spectrum is dominated by a peak at  $\sim 531.8$  eV, which corresponds to adsorbed O<sub>2</sub>, and a weak feature at  $\sim 530.5$  eV, which corresponds to atomic O bound to TiC(001).<sup>34</sup> Thus, only a very small fraction of the adsorbed O<sub>2</sub> dissociates at 150 K. In principle, the O<sub>2</sub> could be bound to the supported Au clusters or to the TiC(001) substrate. The bottom panel in Figure 1 displays Au 4f core-level spectra taken before and after dosing

(37) Perdew, J.; Wang, Y. *Phys. Rev. B* **1992**, *45*, 13244.  
 (38) Bloch, E. *Phys. Rev. B* **1994**, *50*, 17953.  
 (39) Kresse, G.; Joubert, D. *Phys. Rev. B* **1999**, *59*, 1758.  
 (40) Kresse, G.; Hafner, J. *Phys. Rev. B* **1993**, *47*, 558.  
 (41) Kresse, G.; Furthmüller, J. *Phys. Rev. B* **1996**, *54*, 11169.  
 (42) Monkhorst, H. J.; Pack, J. D. *Phys. Rev. B* **1976**, *13*, 5188.  
 (43) Viñes, F.; Sousa, C.; Liu, P.; Rodriguez, J. A.; Illas, F. *J. Chem. Phys.* **2005**, *122*, 174709.  
 (44) Viñes, F.; Illas, F.; Neyman, K. M. *Angew. Chem., Int. Ed.* **2007**, *46*, 7094.  
 (45) Roldán, A.; Ricart, J. M.; Illas, F. *Mol. Simul.* **2009**, *35*, 1051.

(46) Henkelman, K.; Jonson, H. *J. Chem. Phys.* **2000**, *117*, 303.  
 (47) Henkelman, G.; Uberuaga, B. P.; Jonsson, H. *J. Chem. Phys.* **2000**, *113*, 9901.  
 (48) Henkelman, G.; Jónsson, H. *J. Chem. Phys.* **1999**, *111*, 7010.  
 (49) Viñes, F.; Sousa, C.; Illas, F.; Liu, P.; Rodriguez, J. A. *J. Phys. Chem. C* **2007**, *111*, 16982.  
 (50) Zhang, Y. F.; Viñes, F.; Xu, Y. J.; Li, Y.; Li, J. Q.; Illas, F. *J. Phys. Chem. B* **2006**, *110*, 15454.  
 (51) Viñes, F.; Sousa, C.; Illas, F.; Liu, P.; Rodriguez, J. A. *J. Phys. Chem. C* **2007**, *111*, 1307.



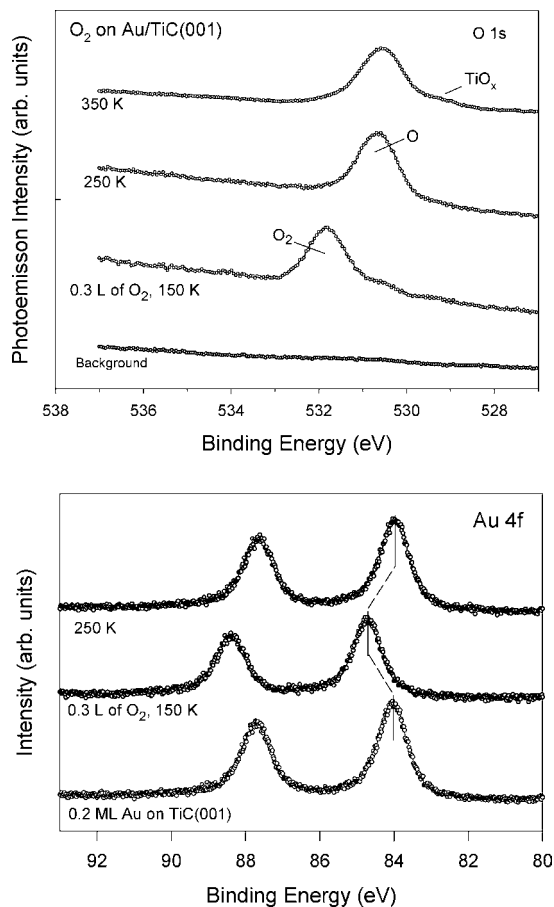


**Figure 1.** O 1s (top panel) and Au 4f (bottom panel) spectra acquired after dosing O<sub>2</sub> to a TiC(001) surface precovered with 0.2 ML of Au. The dosing of O<sub>2</sub> was carried out at 150 K and then the sample was annealed to 250 and 350 K.

O<sub>2</sub> to the Au/TiC(001) surface at 150 K. The adsorption of oxygen induces a positive binding-energy shift of  $\sim 0.7$  eV in the Au 4f spectra, which indicates direct Au $\leftrightarrow$ O<sub>2</sub> bonding interactions. This is clear evidence that a sufficiently large number of O<sub>2</sub> molecules directly interact with the Au nanoparticles. Heating from 150 to 250 K removes the binding-energy shift in the Au 4f peaks and in the O 1s region a strong peak appears at  $\sim 530.7$  eV. This peak is characteristic of atomic O chemisorbed on TiC(001).<sup>34</sup> Thus, the photoemission results indicate that at 150 K O<sub>2</sub> adsorbs molecularly preferentially on the gold nanoparticles, and upon heating to temperatures above 200 K, the O<sub>2</sub>  $\rightarrow$  2O reaction takes place with subsequent migration of atomic oxygen to the TiC(001) substrate. Final heating to 350 K produces minor changes in the O 1s region. A weak feature appears in the range of 529–530 eV, which indicates that there is some exchange of Ti–C and Ti–O bonds with oxidation of the metal carbide.<sup>34</sup> Hence, one probably has some TiO<sub>x</sub> species in the system together with O atoms chemisorbed on TiC(001). For O/TiC(001), images of STM show that at room temperature the oxidation process of the metal carbide is very limited, being mainly localized at the step edges between terraces of the surface.<sup>34</sup>

Previous XPS studies indicate that the C 1s core level of TiC(001) is affected by the adsorption of oxygen.<sup>34,35</sup> This phenomenon is easier to detect with synchrotron-based high-resolution photoemission than with standard XPS. At a photon energy of 380 eV, the emitted electrons have a kinetic energy of 90–95 eV and photoemission probes only the composition

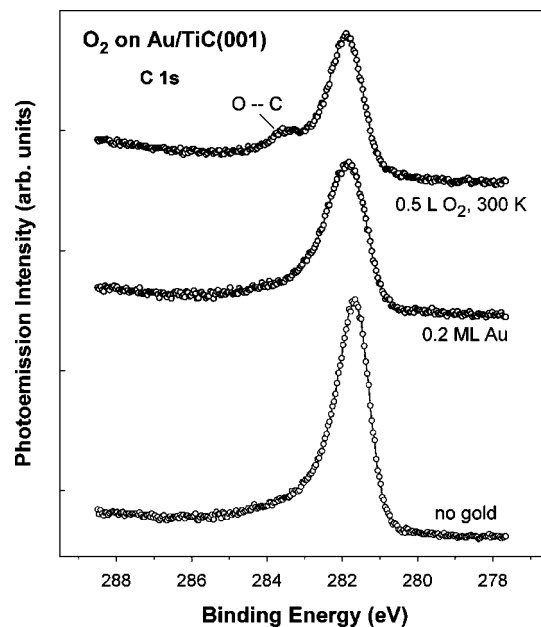


**Figure 2.** C 1s photoemission data for clean TiC(001), Au/TiC(001), and O<sub>2</sub>/Au/TiC(001). A photon energy of 380 eV was used to excite the electrons.

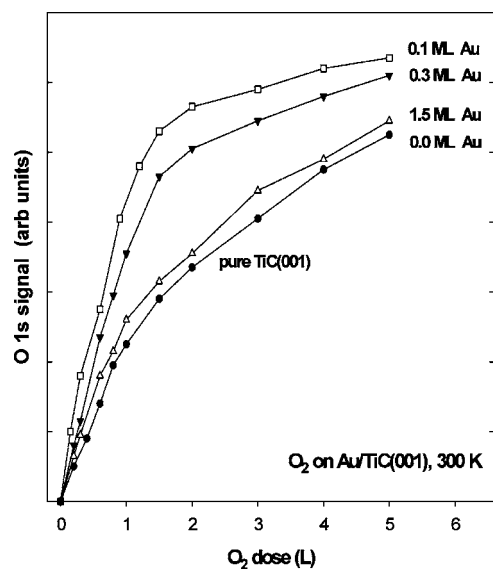
of the first two to three layers in the sample.<sup>52</sup> Figure 2 shows C 1s core level spectra ( $h\nu = 380$  eV) collected after depositing 0.2 ML of Au on TiC(001) and after dosing 0.5 L of O<sub>2</sub> at 300 K. Our spectrum for clean TiC(001) matches the position and line shape of that reported in ref 53. The deposition of Au induces attenuation in the intensity and an increase of  $\sim 60\%$  in the full-width at half-maximum of the C 1s peak. New features appear in the 282–283 eV region as a consequence of Au–C bonding.<sup>31</sup> The C 1s spectrum for O<sub>2</sub>/Au/TiC(001) exhibits a distinctive line shape with a clear peak at  $\sim 283.5$  eV. This peak is also seen in the corresponding C 1s spectrum for O<sub>2</sub>/TiC(001) and denotes bonding of O to C atoms in TiCC hollow sites.<sup>24,36</sup> Thus, the photoemission data in Figures 1 and 2 indicate that at 300 K the atomic oxygen present in a system initially containing O<sub>2</sub>/Au/TiC(001) is mainly bonded to the metal carbide.

Figure 3 compares the uptake of oxygen, O<sub>2,gas</sub>  $\rightarrow$  2O<sub>ads</sub>, of clean TiC(001), and carbide surfaces with 0.1, 0.3, and 1.5 ML of gold. The dosing of O<sub>2</sub> was done at 300 K. The addition of Au clearly enhances the rate of O<sub>2</sub> dissociation on the surface. Although Au facilitates the O<sub>2</sub>(gas)  $\rightarrow$  2O(ads) reaction, we did not find evidence in photoemission for a direct Au–O bonding (at 300 K). The corresponding Au 4f spectra had peak positions similar to those seen in the bottom panel of Figure 1 at 250 K. The experiments of Figure 3 suggest that O<sub>2</sub> probably binds to Au atoms or the gold–carbide interface, the O–O bond breaks apart, and the O atoms end bonded to the TiC(001) substrate. An important conclusion from these experiments is that they clearly show that the reactivity of Au/TiC(001) toward O<sub>2</sub> dissociation is much higher than that of Au/TiO<sub>2</sub>(110) or Au/MgO(001),<sup>11,13,54–57</sup> where the cleavage of O–O bonds is very difficult. This is additional evidence of the extraordinary

(52) Somorjai, G. A. *Chemistry in Two Dimensions: Surfaces*; Cornell University Press: Ithaca, 1981; p 41.

(53) Johansson, L. I.; Johansson, H. I. P.; Håkansson, K. L. *Phys. Rev. B* **1993**, *19*, 14520.

(54) Bondzie, V. A.; Parker, S. C.; Campbell, C. T. *J. Vac. Sci. Technol. A* **1999**, *17*, 1717.



**Figure 3.** Variation of the integrated O 1s signal with O<sub>2</sub> exposure for clean TiC(001) and for Au/TiC(001) surfaces with 0.1, 0.3, and 1.5 ML of gold. The dosing of O<sub>2</sub> was done at 300 K. Under these conditions, only atomic O was present on the surface through O<sub>2,gas</sub> → 2O<sub>ads</sub>.

effect of the TiC support on the catalytic activity of supported Au nanoparticles.<sup>32,33</sup> In Figure 3, it is very important to notice the large effect of the Au coverage on the reactivity of the Au nanoparticles in the Au/TiC(001). The smaller the Au coverage, the larger the Au/TiC(001) reactivity: 1.5 ML of Au ≪ 0.3 ML of Au < 0.1 ML of Au.

Figure 4 shows the distribution of heights observed with STM after depositing 0.1 and 1.5 ML of Au on TiC(001). For a coverage of 0.1 ML of Au, a large fraction of the Au particles exhibits a height of ~0.2 nm with respect to the carbide substrate. These small particles are two-dimensional (i.e., one single Au layer) and have a diameter below 0.6 nm,<sup>32</sup> which would point particles such as planar Au<sub>4</sub> with a diameter 0.4 nm.<sup>31</sup> When the Au coverage is increased to 1.5 ML, one sees a significant increase in the average height of the Au particles, which are mainly three-dimensional (3D). In general, for Au coverages higher than 1 ML, one is dealing with 3D Au particles that have sizes in the range of 1.5–3 nm.<sup>32</sup> The trends in Figure 3 reflect the effect that variations in the height and size of the Au particles have in their chemical activity toward O<sub>2</sub> dissociation. As will be shown below by DF calculations, contact of Au with TiC(001) is essential for charge polarization and an enhancement in the chemical activity of the Au nanoparticle. Thus, small two-dimensional (2D) particles that expose Au atoms in contact with TiC(001) are the most reactive toward O<sub>2</sub>.

**B. Adsorption and Dissociation of O<sub>2</sub> on Au/TiC(001): Density Functional Studies.** Our first-principles calculations for the clean TiC(001) surface gave a geometry that is in very good agreement with that obtained in LEED experiments and other theoretical studies<sup>33</sup> and independent of the unit cell used (e.g., 2 × 2, 3 × 3, 5 × 5, or 6 × 6), as expected. For the interaction of the O<sub>2</sub> molecule with the clean TiC(001) surface, DF

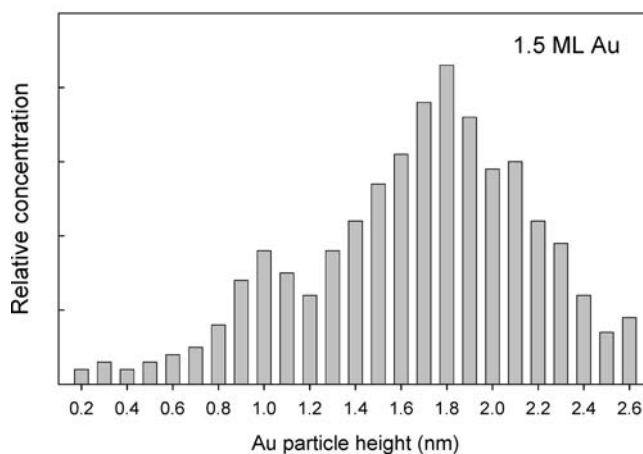
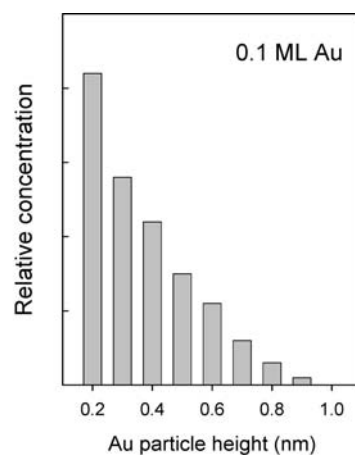


**Figure 4.** Distribution of Au particle heights determined from STM images recorded after depositing 0.1 and 1.5 ML of Au on TiC(001) at 300 K.

calculations show a relatively small but noticeable adsorption energy ( $E_{\text{ads}} \sim 0.45$  eV).<sup>49,50</sup> The molecule is adsorbed with its O–O bond parallel to the surface and the O–O distance increases from 1.23 Å in free O<sub>2</sub> to 1.37 Å in adsorbed O<sub>2</sub>.<sup>49</sup> Here, we examined the bonding of O<sub>2</sub> to TiC(001) surfaces containing a gold monolayer or gold clusters of increasing size (Au<sub>2</sub>, Au<sub>4</sub>, Au<sub>13</sub>, or Au<sub>29</sub>). In the past, we have investigated the interaction of Au<sub>2</sub>, Au<sub>4</sub>, and Au<sub>29</sub> with TiC(001).<sup>31,32</sup> These clusters adsorb via Au–C bonding, leading either to two-dimensional (2D) or three-dimensional (3D) structures.<sup>31,32</sup> The substrate imposes an epitaxial growth, which results in structures with (001)-like facets parallel to the TiC(001) surface. For the 3D clusters, the resulting structure is like a truncated square pyramid with (111) facets in the pyramid faces. It is important to point out that these structures are very different from the octahedral or cubooctahedral shapes predicted by simple Wulff construction and usually seen for Au particles supported on oxides.<sup>58</sup> The origin of this difference is the result of a strong shape-conditioning due to the surface ↔ gold nanoparticle interactions.

On the Au/TiC(001) systems, O<sub>2</sub> is adsorbed with its O–O bond parallel to the surface (see Figure 5) as in clean TiC(001), but the O–O distance is more elongated, reaching a maximum for Au<sub>4</sub> and then decreasing as the particles become 3D (Table 1). This is a first indication that small flat particles are active

(55) Bondzie, V. A.; Parker, S. C.; Campbell, C. T. *J. Catal. Lett.* **1999**, *63*, 143.

(56) Liu, L. M.; McAllister, B.; Ye, H. Q.; Hu, P. *J. Am. Chem. Soc.* **2006**, *128*, 4017.

(57) Stiehl, J. D.; Gong, J.; Ojifinni, R. A.; Kim, T. S.; McClure, S. M.; Mullins, C. B. *J. Phys. B* **2006**, *110*, 20337.

(58) Hashmi, A. S. K.; Hutchings, G. J. *Angew. Chem. Intl. Ed.* **2006**, *45*, 7895.

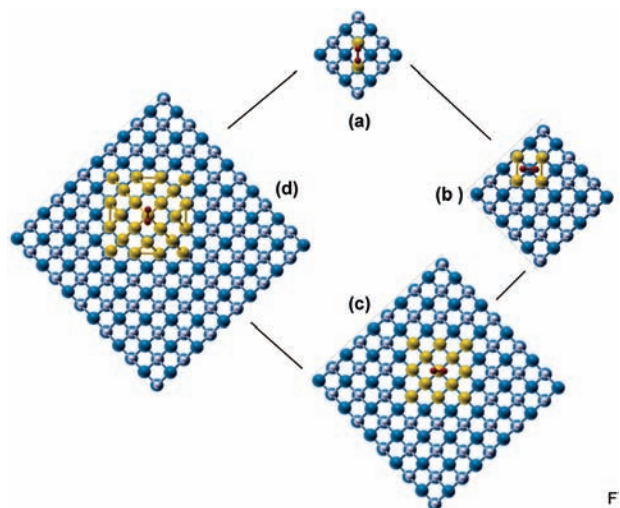


**Figure 5.** Top view for the adsorption of O<sub>2</sub> on (a) Au<sub>2</sub>/TiC(001), (b) Au<sub>4</sub>/TiC(001), (c) Au<sub>13</sub>/TiC, and (d) Au<sub>29</sub>/TiC(001) surfaces. Color code: red (oxygen), yellow (gold), blue (carbon), white (titanium).

toward O<sub>2</sub> dissociation. Indeed, this is consistent with an intermediate value for the O–O distance of O<sub>2</sub> on the supported Au monolayer. Table 1 also lists calculated adsorption energies for the bonding of O<sub>2</sub> to TiC(001) and Au/TiC(001). One can see a clear increase in the adsorption energy of O<sub>2</sub> when going from clean TiC(001) to the Au/TiC(001) systems, which reaches a maximum for Au<sub>4</sub> and then decreases when going to the 3D supported particles up to a more or less constant value that coincides with the case of the Au monolayer. These results are in full agreement with the experimental observation described

**Table 1.** Adsorption Energy ( $E_{\text{ads}}$  in eV) and O–O and O–Au ( $d_{\text{O–O}}$  and  $d_{\text{O–Au}}$  in Å) Distances Properties of O<sub>2</sub> on TiC(001) and on Several Au/TiC(001) Models as Predicted from DF Calculations<sup>a</sup>

system	$E_{\text{ads}}$	$d_{\text{O–O}}$	$d_{\text{O–Au}}$
TiC(001)	–0.58	1.37	—
Au <sub>2</sub> /TiC(001)	–1.80	1.42	2.07
Au <sub>4</sub> /TiC(001)	–1.41	1.55	2.30
Au <sub>13</sub> /TiC(001)	–0.67	1.47	2.27
Au <sub>29</sub> /TiC(001)	–0.97	1.44	2.32
Au <sub>Monolayer</sub> /TiC(001)	–0.99	1.46	2.32

<sup>a</sup> The bonding geometries of O<sub>2</sub> on Au<sub>2</sub>/TiC(001), Au<sub>4</sub>/TiC(001), Au<sub>13</sub>/TiC(001), and Au<sub>29</sub>/TiC(001) are shown in Figure 5.

in section III.A and explains the experimental trends in Figure 1, indicating that there is preferential adsorption of O<sub>2</sub> on the Au sites of a TiC(001) surface partially covered with gold (0.2 ML). It is interesting to compare the adsorption of O<sub>2</sub> on Au<sub>4</sub>/TiC(001) and on Au<sub>29</sub>/TiC(001). In both cases, the O<sub>2</sub> molecule interacts with four gold atoms, which have a low coordination number (see Figure 5). For Au<sub>4</sub>/TiC(001), the gold atoms that are directly in contact with the TiC(001) substrate experience a substantial electron polarization toward the vacuum side.<sup>31,32</sup> This phenomenon favors strong O<sub>2</sub>↔Au bonding interactions with an adsorption energy of –1.41 eV. In the case of Au<sub>29</sub>/TiC(001), the Au atoms interacting with O<sub>2</sub> are not substantially affected by the TiC(001) substrate and one has an adsorption energy of –0.97 eV only. Thus, going from flat 2D particles to larger 3D clusters has a large effect on the adsorption energy and could be anticipated from the O–O distances discussed above. Therefore, the highest reactivity in Table 1 corresponds to small gold clusters that expose Au sites that are in direct

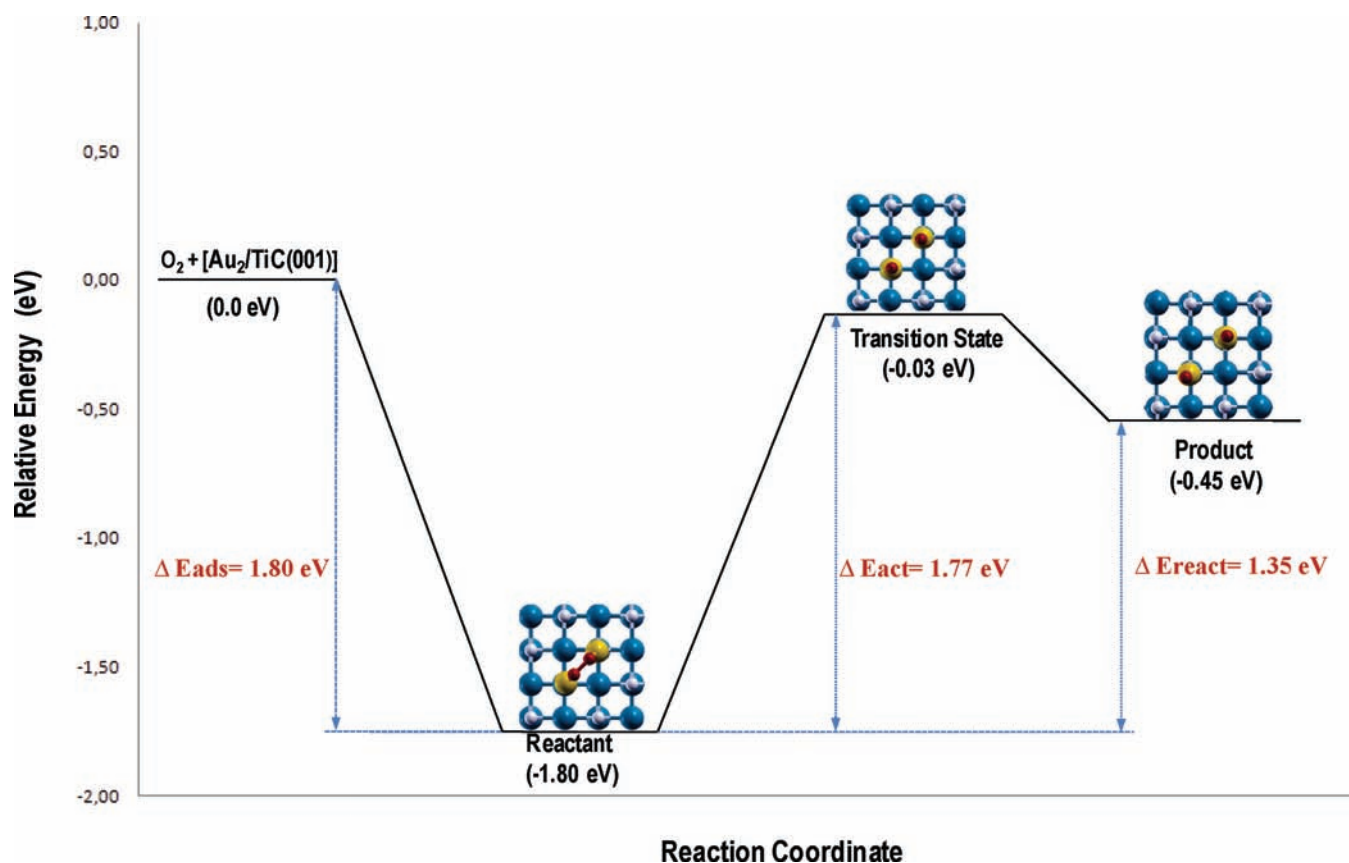


**Figure 6.** Calculated energy profile for the dissociation of O<sub>2</sub> on Au<sub>2</sub>/TiC(001). The color code is as in Figure 5.

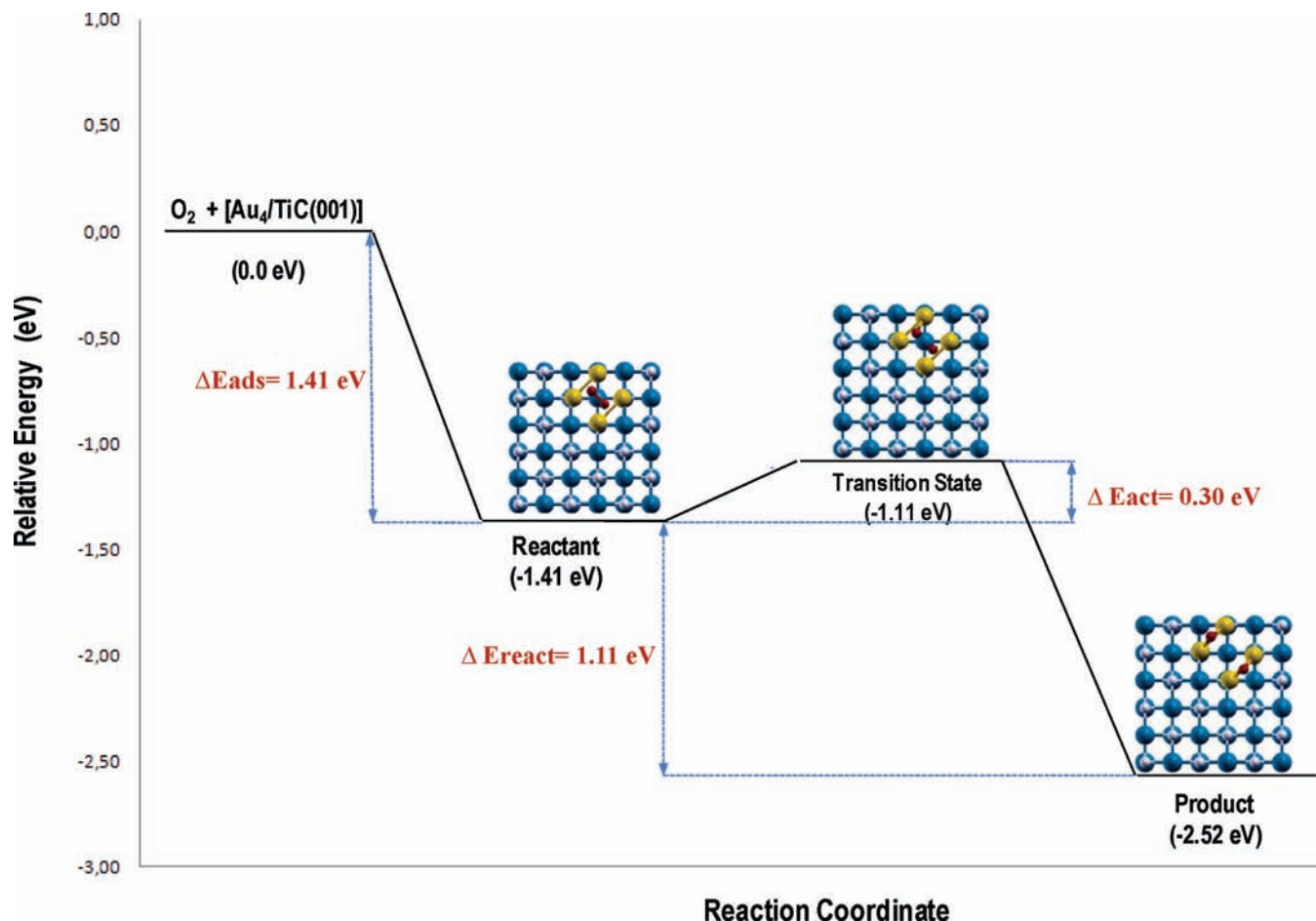


**Figure 7.** Calculated energy profile for the dissociation of O<sub>2</sub> on Au<sub>4</sub>/TiC(001). The color code is as in Figure 5.

contact with the TiC(001) substrate. This is fully consistent with the trends observed in the experimental measurements (Figure 3).

DF calculations for the dissociation of O<sub>2</sub> on unsupported Au clusters show that the presence of low-coordinated Au atoms is not enough to dissociate the molecule.<sup>15,16</sup> Strong adsorption of molecular oxygen on Au nanoparticles is a necessary but not sufficient condition for O<sub>2</sub> dissociation.<sup>15</sup> In general terms, the dissociation of O<sub>2</sub> on free Au nanoparticles<sup>15,16</sup> or on Au nanoparticles supported on MgO(100)<sup>7,13</sup> or TiO<sub>2</sub>(110)<sup>9,11</sup> is a quite difficult reaction. Figures 6–8 display energy profiles calculated for O<sub>2</sub> dissociation on Au<sub>2</sub>/TiC(001), Au<sub>4</sub>/TiC(001), and Au<sub>29</sub>/TiC(001). Although the chemisorption of O<sub>2</sub> on these systems produces a significantly large elongation of the O–O bond (1.42–1.55 Å; see Table 1), there is no spontaneous dissociation of the molecule. Activation barriers prevent the occurrence of the O<sub>2,ads</sub> → 2O<sub>ads</sub> reaction at low temperature (Figure 1). At room temperature, the breaking of the O–O bond occurs, and in this aspect, the Au/TiC(001) systems are more chemically active than Au/MgO(100) and Au/TiO<sub>2</sub>(110) surfaces.<sup>14,16,18,20</sup>

The adsorption energy of O<sub>2</sub> on Au<sub>2</sub>/TiC(001) is the highest in Table 1, but the O<sub>2,ads</sub> → 2O<sub>ads</sub> reaction has a large activation barrier (~1.8 eV) and is an endothermic process (ΔE = 1.35 eV). The Au<sub>2</sub> dimer supported on TiC(001) is not able to accommodate well the two oxygen atoms produced by the dissociation of O<sub>2</sub> and it is too small to allow oxygen dissociation. On the other hand, Au<sub>4</sub> can bind well two oxygen atoms and the Au<sub>4</sub>/TiC(001) system is excellent for adsorbing

and dissociating O<sub>2</sub> (Figure 7). On Au<sub>4</sub>/TiC(001), the barrier for the dissociation of O<sub>2</sub> is only 0.30 eV and the O<sub>2,ads</sub> → 2O<sub>ads</sub> reaction is very exothermic (ΔE = –1.11 eV). Moving from 2D to 3D particles, as expected upon Au coverage increase, has a clear effect on the overall energy profile, e.g. adsorption and activation energy to break the O–O bond; see Table 2. Thus, dissociation of O<sub>2</sub> on the supported Au<sub>13</sub> nanoparticle has an activation energy of 0.57 eV, still rather low but significantly larger than the 0.30 eV energy barrier predicted for the supported Au<sub>4</sub> particle (Table 2). Note that the increase in the dissociation energy barrier from Au<sub>4</sub> to Au<sub>13</sub> is accompanied with a decrease on the adsorption energy. As a result, oxygen molecules adsorb less on the 3D Au<sub>13</sub> nanoparticle and are harder to dissociate, or in other words, the catalytic activity of the supported Au<sub>13</sub> is significantly lower than that of the supported 2D Au<sub>4</sub> particle. This conclusion is fully supported by the calculations carried out for supported Au<sub>29</sub>, which is the largest particle studied in the present work. Au<sub>29</sub>/TiC(001) adsorbs O<sub>2</sub> slightly better than Au<sub>13</sub> but worse than Au<sub>4</sub>, this is because these particles have a size that is far from the scalable regime, and hence, every atom counts. Similarly, Au<sub>29</sub>/TiC(001) is able to dissociate the molecule (Figure 8), but it is not as reactive as Au<sub>4</sub>/TiC(001) (Figure 8). The decrease of adsorption energy and increase of activation energy with increasing particle size is also consistent with a decrease in the exothermicity of the O<sub>2,ads</sub> → 2O<sub>ads</sub> reaction, which decreases from –1.11 to –0.97 eV when going from Au<sub>4</sub>/TiC(001) to Au<sub>29</sub>/TiC(001). For particles larger than



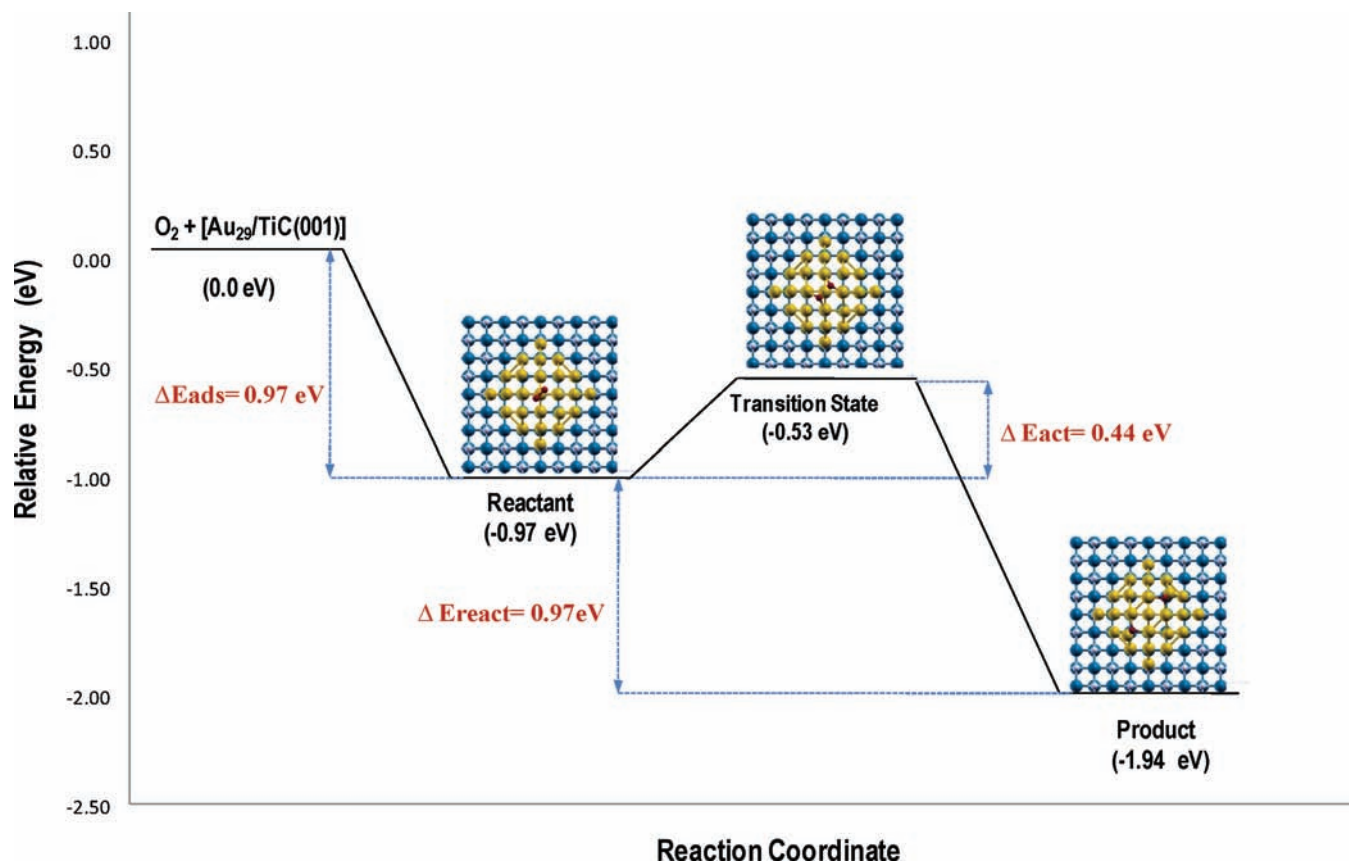


**Figure 8.** Calculated energy profile for the dissociation of  $O_2$  on  $Au_{29}/TiC(001)$ . The color code is as in Figure 5.

**Table 2.** Activation Energy ( $E_{act}$  in eV), O–O and O–Au ( $d_{O-O}$  and  $d_{O-Au}$  in Å) Distances of the Transition State Structures Corresponding to  $O_2$  Dissociation on the Different Au/TiC(001) Models Used in the Present Work

system	$E_{act}$	$d_{O-O}$	$d_{O-Au}$
$Au_2/TiC(001)$	1.77	2.78	1.88
$Au_4/TiC(001)$	0.30	1.87	2.19
$Au_{13}/TiC(001)$	0.57	2.12	2.10
$Au_{29}/TiC(001)$	0.44	1.98	2.06
$Au_{Monolayer}/TiC(001)$	0.23	1.81	2.19

$Au_{29}$ , one rapidly approaches the scalable regime,<sup>59</sup> the influence of the particle size is likely to become less marked, and one can safely conclude that DF calculations predict that 2D particles are more reactive than 3D ones, in full agreement with the experimental observations reported in the previous section.

The theoretical results in Figures 7 and 8 highlight the importance of having small 2D gold clusters that expose Au sites that are in direct contact with the TiC(001) substrate. To further confirm that 2D Au clusters supported on TiC(001) exhibit a particular catalytic activity, related to the polarization of the Au atoms electron density by the underlying substrate, we consider the limiting case of a Au monolayer. On this extended Au system, the  $O_2$  adsorption energy is close to that of the  $Au_{29}/TiC(001)$  system (Table 1), the lower value of the adsorption energy being caused by the lack of edge atoms. The same effect causes a slight decrease of the exothermicity of the reaction from  $-1.11$  eV for  $Au_4/TiC(001)$  to  $-1.02$  eV for the supported Au monolayer. However, this decrease in adsorp-

tion capability is not enough to make the Au monolayer inactive toward  $O_2$  dissociation. On the contrary, the activation energy for this reaction (Table 2) is 0.23 eV, very close and slightly smaller than the value calculated for the  $Au_4/TiC(001)$  system. This model system nicely illustrates the important effect of the underlying TiC(001) substrate on the chemistry of the supported Au nanoparticles. To further reinforce this point note that the predicted barrier for  $O_2$  dissociation on Au(111) is at least 1.5 eV.<sup>60</sup>

To complete the comparison to experiment, Figure 9 shows the calculated energy profile for the diffusion of O atoms in  $Au_4/TiC(001)$  from the Au cluster to the TiC(001) terrace. The migration of O from above the  $Au_4$  to the metal carbide substrate is a highly exothermic process with an exothermicity that goes from 0.95 to 1.07 eV, depending on whether the O atoms sit above TiC sites close or far from the Au cluster. Thus, while the  $O_2$  molecule prefers binding to Au sites (see Table 1), the O atoms interact more strongly with the TiC(001) surface. However, the O migration step is an activated process with an energy barrier of 0.7 eV. Note that the theoretical calculations agree with the model proposed above to explain the photoemission data of Figures 1 and 2: At low temperatures  $O_2$  adsorbs molecularly on the gold nanoparticles, and upon heating to room temperature, the  $O_{2,ads} \rightarrow 2O_{ads}$  reaction takes place with eventual migration of atomic oxygen to the TiC(001) substrate. The reaction pathways shown in Figure 9 eventually will lead to oxidation of the metal carbide surface through exchange of Ti–C and TiO bonds at elevated temperatures.<sup>34</sup> At temperatures below 250 K, the oxygen will have a significant lifetime on the Au nanoparticles, opening the route for many chemical reactions

(59) Roldán, A.; Viñes, F.; Illas, F.; Ricart, J. M.; Neyman, K. M. *Theor. Chem. Acc.* **2008**, *120*, 565.

(60) Torres, D.; Illas, F. *J. Phys. Chem. B* **2006**, *110*, 13310.



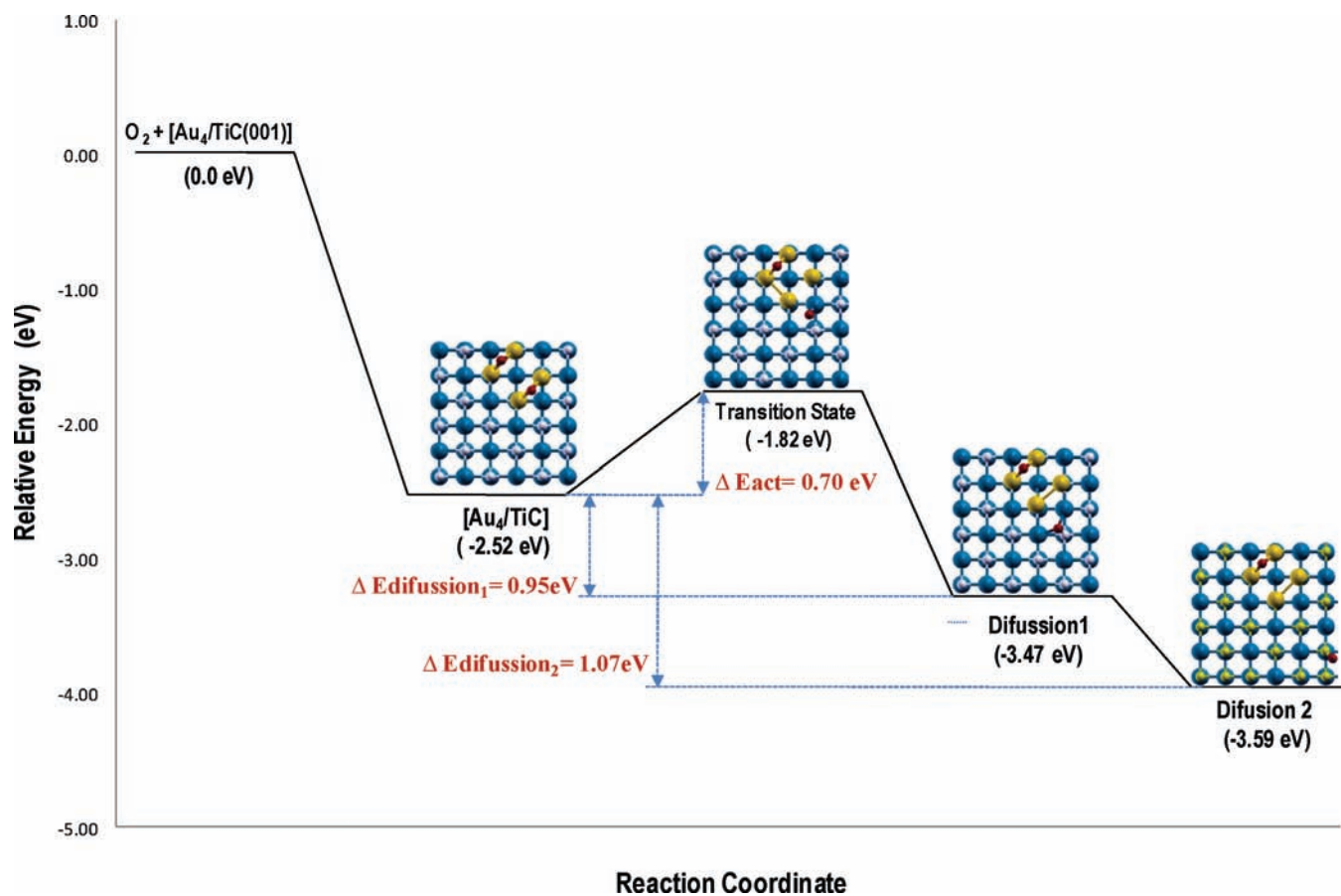


**Figure 9.** Calculated energy profile for the migration of atomic oxygen on a Au<sub>4</sub>/TiC(001) system. Initially, two oxygen atoms are bonded to the Au<sub>4</sub> cluster. The color code is as in Figure 5.

seen on O/Au(111).<sup>4–10</sup> Thus, the O<sub>2</sub>/Au/TiC(001) or O/Au/TiC(001) systems should react with with CO, CO<sub>2</sub>, NH<sub>3</sub>, H<sub>2</sub>O, CH<sub>3</sub>OH, CH<sub>3</sub>CH<sub>2</sub>OH, and CH<sub>3</sub>CH<sub>2</sub>CH<sub>2</sub>OH.<sup>4–10</sup>

The discussion above makes it clear that experiment and theory show that O<sub>2</sub> can easily dissociate on Au nanoparticles supported on TiC(001) and that 2D particles are more active. From previous work on isolated cuboctahedral particles, we know that there is a critical particle size for O<sub>2</sub> dissociation, but nothing is known about the reactivity of isolated Au particles similar to those found above the TiC(001) support.<sup>23</sup> In part, this is because particles with the shape imposed by the underlying support are either not stable when isolated or represent an energetically unfavorable isomer. It is tempting to suggest that the special reactivity of the Au nanoparticles supported on TiC(001) is due to a combination of the shape imposed by the substrate and the subsequent charge polarization also provoked by the substrate.

**C. Consequences for CO Oxidation on Au/TiC(001).** It has been reported that Au nanoparticles dispersed on TiC films can oxidize carbon monoxide ( $2\text{CO} + \text{O}_2 \rightarrow 2\text{CO}_2$ ) at temperatures below 200 K.<sup>30,61</sup> What type of oxygen species participate in the key steps for the  $2\text{CO} + \text{O}_2 \rightarrow 2\text{CO}_2$  reaction: molecular O<sub>2</sub> or atomic O? We carried out TDS experiments after dosing CO to the different systems shown in Figure 1. In a set of experiments, 0.3 L of O<sub>2</sub> was dosed to the Au/TiC(001) surface at 150 K. The sample containing chemisorbed O<sub>2</sub> was cooled down to 100 K and exposed to 0.6 L of CO, and the evolution

of CO<sub>2</sub> was monitored with a mass spectrometer while the sample temperature was increased from 100 to 300 K. Desorption of CO<sub>2</sub> was observed at temperatures between 140 and 160 K. In a second set of experiments, 0.3 L of O<sub>2</sub> was dosed to the Au/TiC(001) surface at 150 K with subsequent heating to 300 K to produce atomic oxygen. The sample containing chemisorbed atomic O was cooled down to 100 K and exposed to 0.6 L of CO, and then the temperature was increased from 100 to 300 K. In this case, the amount of CO<sub>2</sub> that evolved from the surface was negligible. These experiments provide strong evidence that the oxygen species active during the low-temperature oxidation of carbon monoxide on Au/TiC(001) is chemisorbed O<sub>2</sub>, as occurs in the case of Au/oxide surfaces.<sup>14,18,20</sup> Note also that once atomic O binds to TiC(001), the chemisorption bond is so strong that temperatures well above 400 K are necessary to remove the O adatoms by direct reaction with CO.

The theoretical results in Table 1 show a quite large elongation (0.2–0.3 Å) in the O–O bond of O<sub>2</sub> upon adsorption of the molecule on Au/TiC(001). The weakened O–O bond can be easily broken by interactions with CO or other molecules (CO<sub>2</sub>, NH<sub>3</sub>, H<sub>2</sub>O, ROH, etc.). Calculations need to be carried out to explore the possibility of  $\text{O}_{2,\text{ads}} + 2\text{CO}_{\text{ads}} \rightarrow 2\text{CO}_{2,\text{gas}}$  or  $\text{O}_{\text{ads}} + \text{CO}_{\text{ads}} \rightarrow \text{CO}_{2,\text{gas}}$  reactions before oxygen migrates from Au sites to the TiC(001) surface. From previous work, we know that the adsorption energy of CO on the oxidized carbide<sup>34</sup> is close to those calculated and measured experimentally for CO on pure TiC(001), –0.4 and –0.5 eV,<sup>62,63</sup> respectively. The CO molecule would desorb from TiC(001) at temperatures

(61) Ono, L. K.; Roldan Cuenya, B. *Catal. Lett.* **2007**, *113*, 86.

above 250 K,<sup>63</sup> and thus, it could not prevent the oxidation of the carbide substrate when Au/TiC systems are exposed to mixtures of CO/O<sub>2</sub> at temperatures above 300 K. Therefore, a long-term Au/TiC catalyst for the 2CO + O<sub>2</sub> → 2CO<sub>2</sub> reaction with good performance is foreseen at low temperatures only.

#### IV. Summary and Conclusions

High-resolution photoemission and density functional calculations on realistic slab models were used to study the interaction of O<sub>2</sub> with Au nanoparticles supported on TiC(001). After dosing molecular oxygen to a TiC(001) surface precovered with 0.2 ML of Au at 150 K, the O 1s region is dominated by a peak at ~531.8 eV, which corresponds to adsorbed O<sub>2</sub>. The adsorption of oxygen induces a positive binding-energy shift of ~0.7 eV in the Au 4f spectra, which indicates direct Au↔O<sub>2</sub> bonding interactions. The photoemission results indicate that at 150 K O<sub>2</sub> adsorbs molecularly on the gold nanoparticles, and upon heating to temperatures above 200 K, the O<sub>2</sub> → 2O reaction takes place with migration of atomic oxygen to the TiC(001) substrate. A big positive shift (~1.8 eV) was detected for the C 1s core level in photoemission studies, indicating the existence of strong O↔C interactions. Atomic oxygen is present on the Au/TiC(001) surfaces after dosing O<sub>2</sub> at room temperature. The addition of Au to TiC(001) substantially enhances the rate of O<sub>2</sub> dissociation. An important conclusion from the experimental measurements is that the reactivity of Au/TiC(001) toward O<sub>2</sub> is much larger than that of Au/TiO<sub>2</sub>(110) or Au/MgO(001), where the cleavage of O–O bonds is very difficult.

DF calculations carried out on realistic models containing up to 600 atoms lead to a picture of the dissociation process which is in full agreement with the experimental results and shed light on these fascinating results. In particular, the DF calculations show that, in part, the amazing reactivity of the Au/TiC toward molecular oxygen dissociation comes from the shape imposed by the underlying substrate. However, once supported, contact of Au with TiC(001) is essential for charge

polarization and thus for the overall chemical activity of the supported Au nanoparticles. Small two-dimensional particles that expose Au atoms in contact with TiC(001) are the most reactive with rather small energy barriers for O<sub>2</sub> dissociation while larger three-dimensional supported particles tend to exhibit a less marked activity toward O<sub>2</sub> dissociation and larger energy barriers. The O<sub>2</sub> molecule exhibit a clear preference to bind Au sites, whereas the O atoms interact more strongly with the TiC(001) surface, although migration of atomic O from the Au sites to the TiC(001) terrace requires overcoming an energy barrier of ~0.7 eV.

The present study indicates that the oxygen species active during the low-temperature (<200 K) oxidation of carbon monoxide on Au/TiC(001) is likely to be chemisorbed O<sub>2</sub>. This is because once atomic O binds to TiC(001), the chemisorption bond is so strong that temperatures well above 400 K are necessary to remove the O adatoms by direct reaction with CO. DF calculations show a quite large elongation (0.2–0.3 Å) in the O–O bond of O<sub>2</sub> upon adsorption of the molecule on Au clusters in contact with TiC(001). The weakened O–O bond can be easily broken by interactions with CO or other molecules (CO<sub>2</sub>, NH<sub>3</sub>, H<sub>2</sub>O, ROH, etc.)

**Acknowledgment.** The authors are grateful to B. Roldán-Cuenya (University of Central Florida) and J. Gomes (Universidade do Porto) for thought-provoking discussions about the properties of Au/TiC. The research carried out at BNL was supported by the US Department of Energy, Chemical Sciences Division. J.A.R. acknowledges the support of the Generalitat de Catalunya in a visit to the Universitat de Barcelona (2006PIV009). L.F. is grateful to ICyTDF for a Postdoctoral Fellowship. K.N. is grateful to the Nippon Foundation for Materials Science for grants that made possible part of this work, and F.I. acknowledges financial support through Spanish MICINN grant FIS2008-02238/FIS and partial support from Generalitat de Catalunya grants 2009SGR1041 and XRQTC. Generous allocation of computational time on the Marenostrum supercomputer of the Barcelona Supercomputing Center is gratefully acknowledged.

JA910146G

(62) Liu, P.; Rodríguez, J. A. *J. Chem. Phys.* **2004**, *120*, 5414.

(63) Didziulis, S. V.; Frantz, P.; Fernandez-Torres, L. C.; Guenard, R. L.; El-bjeirami, O.; Perry, S. S. *J. Phys. Chem. B* **2001**, *105*, 5196.